Effect of heat treatment on structure and magnetic properties of the Fe–N and Fe–Ti–N alloy films

Article *in* Journal of Alloys and Compounds · August 1997

Impact Factor: 3 · DOI: 10.1016/S0925-8388(97)00049-2

3 authors, including:

Dong-Liang Peng
Xiamen University
178 PUBLICATIONS **2,045** CITATIONS

SEE PROFILE

ELSEVIER

Journal of Alloys and Compounds 259 (1997) 1–6

Journal of ALLOYS AND COMPOUNDS

Effect of heat treatment on structure and magnetic properties of the Fe–N and Fe–Ti–N alloy films

Dong-Liang Peng*, Kenji Sumiyama, Kenji Suzuki

Institute for Materials Research, Tohoku University, Sendai 980, Japan

Accepted 19 September 1996

Abstract

Fe–N and Fe–Ti–N alloy films have been prepared by reactive sputtering. The structure and magnetic properties of the Fe–Ti–N and Fe–N films have been studied as a function of the N_2 flow rate $R(N_2)$ and annealing temperature T_A by X-ray diffraction (XRD) and a vibrating sample magnetometer. The as-prepared and annealed Fe–N films consist of the α-Fe and Fe_4N phases but the Fe–Ti–N films are composed of the α-Fe and Ti_2N phases. The coercivity, H_c, of the Fe–N films changes drastically with $R(N_2)$ and T_A, while that of the Fe–Ti–N films does not change with T_A up to 500 °C. These results indicate that the addition of Ti suppresses the formation of iron nitride phases and improves the thermal stability of Fe–N films. © 1997 Elsevier Science S.A.

Keywords: Structure; Magnetic properties; Sputter-deposition; Annealing; Fe–N film; Fe–Ti–N film

1. Introduction

Much attention has been paid to Fe–N films because of their excellent magnetic properties and the significant improvement of corrosion- and wear-resistance in comparison with pure iron [1–7]. Soft magnetic properties of Fe–N films were ascribed to reduction of grain size and decrease of magnetic anisotropy dispersion, caused by addition of a small amount of nitrogen [8]. However, Fe–N films show high magnetostriction and poor thermal stability, and their good soft magnetic properties disappear with increases in the heating temperature owing to grain growth of the refined iron. Recently, the addition of third elements to form ternary Fe–M–N systems (M= Ta,Zr,Hf,Nb,.....) [9–13] has succeeded in overcoming these weak points. The effects of a small mount of Ti doping to Fe–N [14] and Fe–Co–N [15] films on soft magnetic properties and magnetostriction have been investigated. However, the magnetic properties of Fe–N and Fe–Ti–N alloy films with relatively large amount of Ti and N have not been reported.

In this study, the Fe–N and Fe–Ti–N alloy films were prepared on a water-cooled substrates by a facing-target-type DC sputtering (FTS) system at different nitrogen flow ratios $R(N_2)$, and then as-prepared films were annealed at various temperatures. The change of the structure and magnetic properties after annealing have been investigated.

2. Experimental

Fe–N and Fe–Ti–N alloy films were deposited on glass substrates by the FTS system in a mixed $Ar+N_2$ plasma, using a composite target consisting of pure Fe (99.9%) and Ti (99.9%) plates. The Fe and Ti concentration ratio was adjusted by changing the ratio of the surface area of Fe and Ti plates: the ratio of the surface area is Fe:Ti=7:3 in this study. In order to obtain Fe–Ti–N films with various nitrogen contents the relative N_2 flow rate, $R(N_2)$=[N_2-flow rate]/[Ar-flow rate+N_2-flow rate] (in %), was adjusted by fine control of mass flow meters of N_2 and Ar gas. The substrate during the sputtering deposition was kept at about 50 °C by indirect water cooling. The sputtering conditions are listed in Table 1. The chemical composition (listed in Table 2) of deposited films was determined by inductively coupled plasma (ICP) optical emission spectrometry and helium carrier fusion-thermal conductivity methods. The annealing of as-prepared films is carried out in a vacuum (5×10^{-5} Torr) between 200 and 600 °C for 1 h, where the heating and cooling rates are 5 °C min^{-1}.

Structures of the films were analyzed by X-ray diffrac-

*Corresponding author.

0925-8388/97/$17.00
PII S0925-8388(97)00049-2

Table 1
Sputtering condition

Background pressure	$<4\times10^{-4}$ Pa
Total pressure	9.3×10^{-1} Pa
Nitrogen flow ratio	0~30%
Input power	0.95 kW
magnetic field	
At the target center	8 kAm^{-1}
At the target edge	12 kAm^{-1}
Substrate temperature	Water cooling
Substrate	Glass and polyimide
Deposition rate	~1.0 nm s^{-1}

tion with CuKa radiation using a graphite monochromator. Magnetic properties of the films were measured by a vibrating sample magnetometer (VSM) in a magnetic field up to 10 kOe applied parallel to the plane of the films in the temperature range of 0~900 °C.

3. Results

3.1. Structure

Fig. 1 shows X-ray diffraction patterns of the Fe–Ti–N and Fe–N films sputter-deposited under the same deposition conditions (see Table 1) using the Fe–Ti composite target or Fe target. For Fe–Ti–N films (Fig. 1(a)), the (110) peaks shift to a lower 2θ side (the lattice expands). Broadening of diffraction peaks indicates a tendency of amorphous phase formation and/or refinement of crystal grains as $R(N_2)$ increases. In the Fe–N films (Fig. 1(b)), no γ′-Fe_4N phase is formed at $R(N_2)=10\%$ but formed evidently at $R(N_2)=20$ and 30%. Moveover, the different preferred-orientation of the γ′-Fe_4N phase in two films is observed.

The X-ray diffraction patterns of the Fe–N films annealed at $T_A=400$ °C for 1 h are shown in Fig. 2. The amount and the grain size of γ′-Fe_4N phase increases, comparing with the as-prepared films (Fig. 1(b)).

Fig. 3 shows the X-ray diffraction patterns of the Fe–Ti–N films deposited at $R(N_2)=30\%$ after annealing at

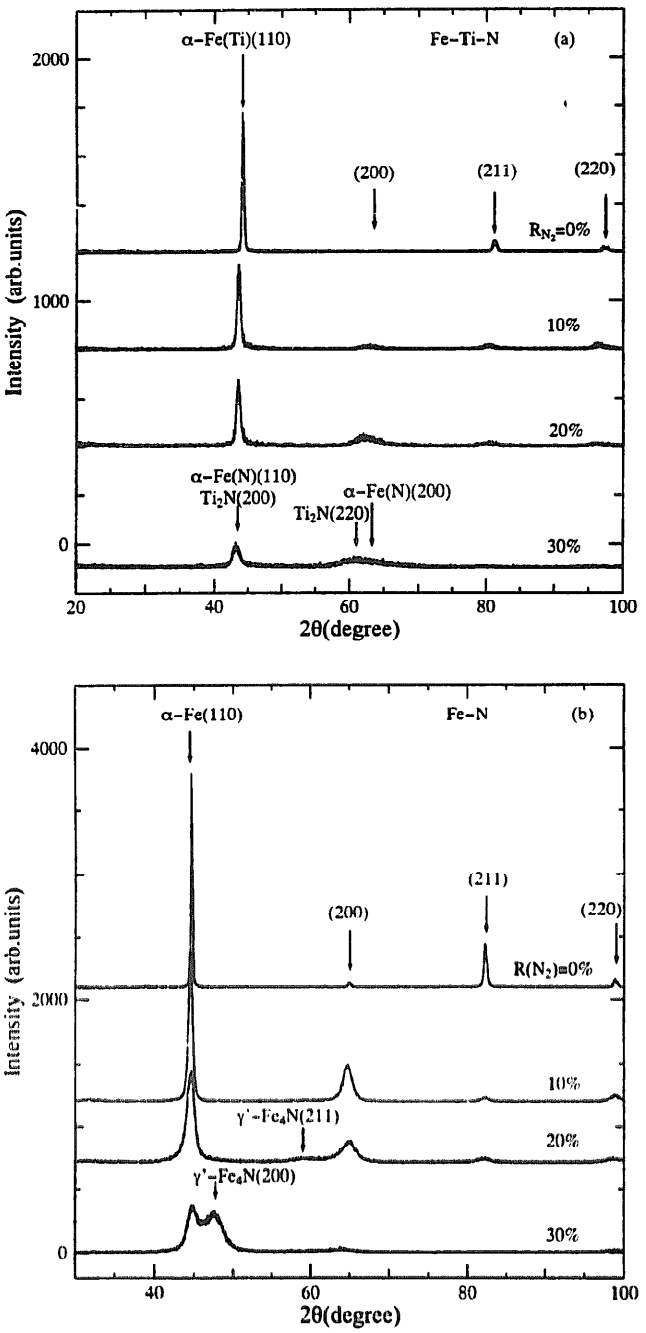

Fig. 1. X-ray diffraction patterns of the Fe–Ti–N (a) and Fe–N (b) films deposited on water-cooled substrates at $R(N_2)=0$, 10, 20 and 30%.

Table 2
Composition analysis results of the Fe–N and Fe–Ti–N films

Target	$R(N_2)$ (%)	Fe (at.%)	Ti (at.%)	N (at.%)
Fe	0	100		
	10	98.1		1.9
	20	94.5		5.5
	30	87.1		12.9
Fe:Ti=7:3	0	89.7	10.3	
	10	88.6	8.3	3.1
	20	87.1	7.0	5.9
	30	83.9	4.9	11.2

$T_A=400$, 500 and 600 °C for 1 h. The annealed films are composed of the α-Fe and Ti_2N phases. The increase in the intensity and sharpness of the diffraction peaks clearly indicate that the large α-Fe grain is formed after the annealing at $T_A>500$ °C.

The lattice constants, a, calculated from the interplanar distance, d_{110}, of α-Fe(110) are plotted versus $R(N_2)$ in Fig. 4 for as-prepared and annealed Fe–Ti–N and Fe–N films. The values of a of the Fe–Ti–N films are always larger than those of pure Fe and Fe–N films. They increase

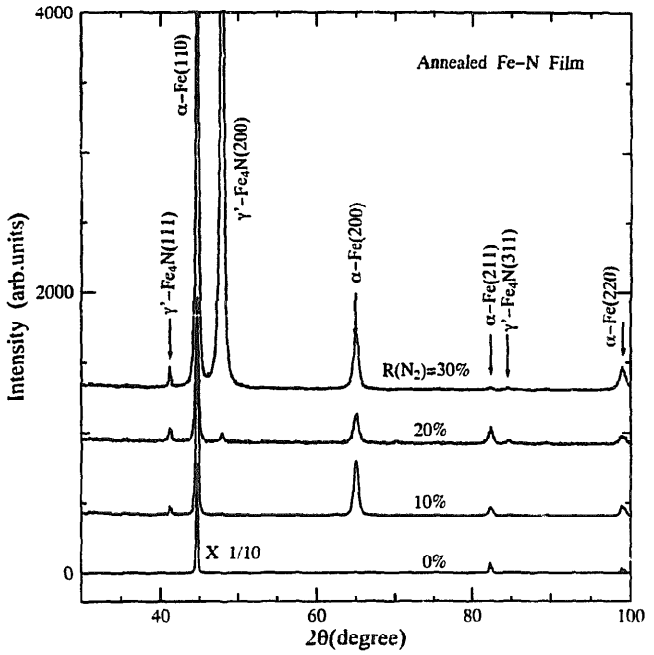

Fig. 2. X-ray diffraction patterns of the Fe–N films annealed at 400 °C for 1 h.

with increasing $R(N_2)$. Moreover, The a values of the annealed Fe–Ti–N films decrease, being accompanied by the grain growth. For the as-prepared Fe–N films, the lattice constant first increases slightly because of the expansion of *bcc*, and then decreases because of the phase transformation from the α-Fe phase to the α′ phase with increasing $R(N_2)$ [17]. After annealing at 400 °C, there are the same a values for all Fe–N films due to growth of the α-Fe grain size, phase transformation from the α′ phase to the *bcc* phase and formation of the γ′-Fe_4N phase.

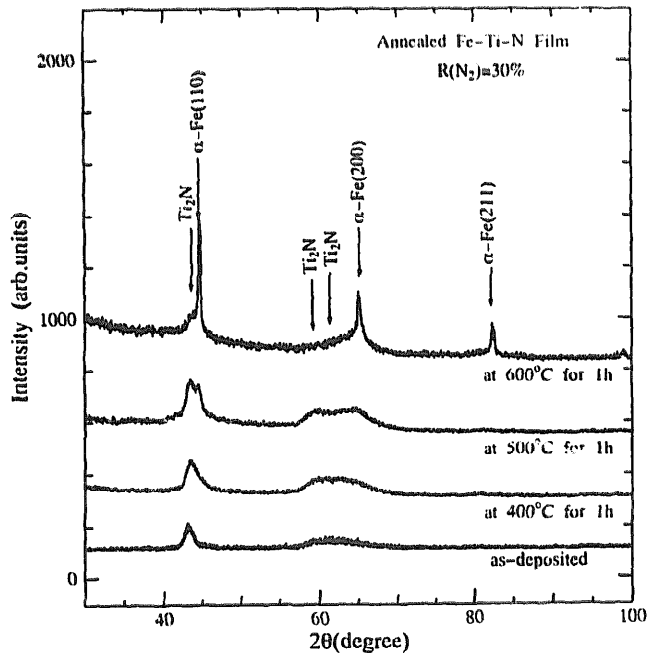

Fig. 3. The change of X-ray diffraction patterns of the Fe–Ti–N films deposited at $R(N_2)=30\%$ with the annealing temperature as a parameter.

3.2. Temperature dependence of magnetic properties

Fig. 5(a) and (b) show the saturation magnetization, M_s, and coercivity, H_c, for the as-prepared and 400 °C annealed Fe–Ti–N and Fe–N films as a function of $R(N_2)$. From Fig. 5(a), the M_s values of the annealed Fe–Ti–N films deposited at $R(N_2)=10$ and 20% are larger than those of the as-prepared films, while there is no change in M_s for $R(N_2)=0$ and 30%. No evident change in H_c can be observed for all Fe–Ti–N films before and after annealing. The H_c first decreases and then increases with increasing $R(N_2)$. For the as-prepared Fe–N films (Fig. 5(b)), the M_s first increases slightly and then decreases with increasing $R(N_2)$. The increase in M_s is ascribable to the expansion of the α-Fe lattice owing to the incorporation of N atoms and the decrease to formation of the γ′-Fe_4N phase [6,7]. The M_s values of the annealed Fe–N films deposited at $R(N_2)=10$ and 20% are smaller than those of the as-prepared films but there is no change in M_s for $R(N_2)=0$ and 30%. This means that transformation from the α′ phase to the *bcc* phase and formation of the γ′-Fe_4N phase after annealing give a same contribution to M_s for the Fe–N film deposited at $R(N_2)=30\%$. The H_c values of the as-prepared Fe–N films increase as increasing $R(N_2)$: $H_c=90$ Oe for $R(N_2)=30\%$. This can be considered as the occurrence of lattice distortion in the films due to incorporation of nitrogen atoms. It is further confirmed by the decrease in H_c of the annealed Fe–N films. The annealed Fe–N films have a about same H_c value.

Fig. 6(a) and (b) show the temperature dependence of magnetization for the Fe–Ti–N and Fe–N films in a magnetic field of 5 kOe. Fig. 6(a) indicates that there are two magnetic transformation in the Fe–Ti–N film for $R(N_2)=0\%$, and the Curie temperature, $T_c=703$ and 540 °C, respectively, while $T_c=730$ °C for the Fe–Ti–N films deposited at $R(N_2)=10$, 20 and 30%. In contrast to the Fe–Ti–N films, the temperature dependence of magnetization for Fe–N films is more complicated (as shown in Fig. 6(b)). The highest T_c value is about 746 °C and there is a magnetic transformation at about 440 °C because of existence of the γ′-Fe_4N phase in the films. Moreover, for the Fe–N film deposited at $R(N_2)=30\%$, the magnetization disappears suddenly in the temperature range from 580 to 680 °C due to phase transformation from *bcc* α-Fe to *fcc* γ-Fe and the decomposition of the γ′-Fe_4N phase at about 570 °C. Although the Fe–N equilibrium phase diagram predicts that decomposition temperature of the γ′-Fe_4N phase is about 680 °C, the lower temperature decomposition is probably due to instability of the non-equilibrium Fe–N films.

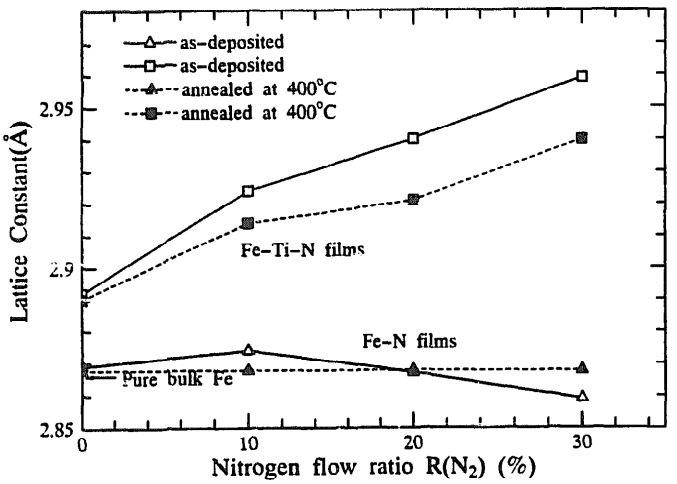

Fig. 4. The change of lattice constant before and after annealing at 400 °C for the Fe–Ti–N and Fe–N films deposited at $R(N_2)$=0, 10, 20 and 30%.

4. Discussion

Fig. 1(a) indicates that Ti atoms apparently dissolve substitutionally and nitrogen atoms interstitially in bcc Fe lattices below $R(N_2)$=20%. At $R(N_2)$=30%, the very broad X-ray diffraction peaks obviously suggest formation of a second phase. The previous X-ray photoelectron spectroscopy (XPS) results have showed that the broad (110) peak for the Fe–Ti–N film deposited at $R(N_2)$=30% is allotted to the α-Fe phase with a very small grain size and the TiN_x phase [16]. It has been proved further that the TiN_x phase is the Ti_2N phase through the change in

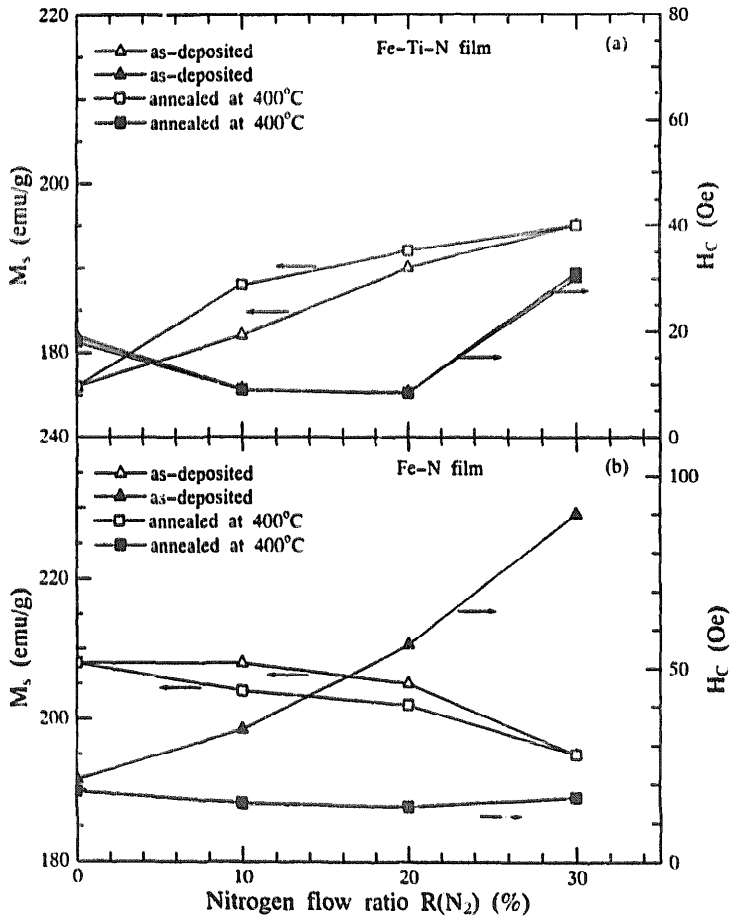

Fig. 5. Variation of saturation magnetization M_s and coercivity H_c before and after annealing at 400 °C for the Fe–Ti–N (a) and Fe–N (b) films deposited at $R(N_2)$=0, 10, 20 and 30%.

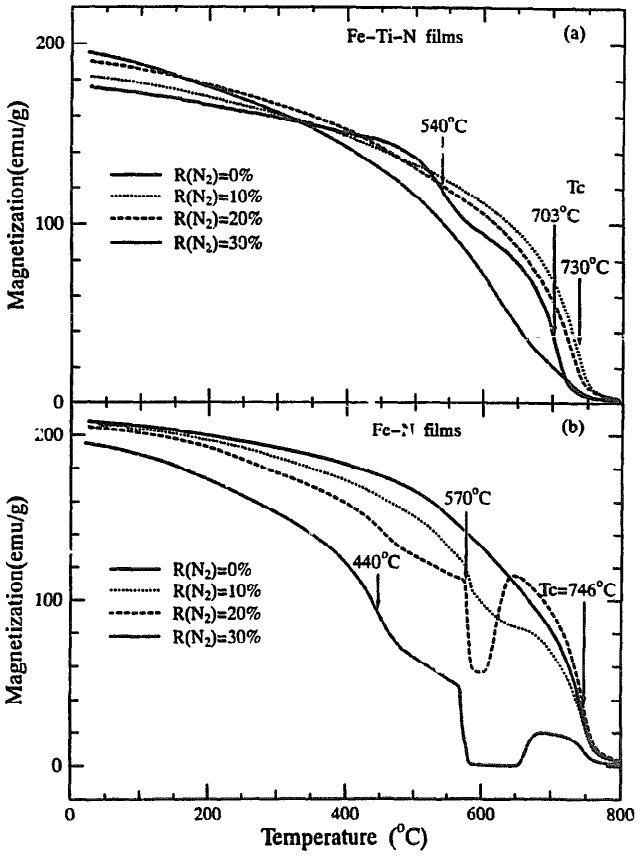

Fig. 6. Heating curves of magnetization for the Fe–Ti–N for the Fe–Ti–N (a) and Fe–N (b) films deposited at $R(N_2)=0$, 10, 20 and 30% in a magnetic field of 5 kOe.

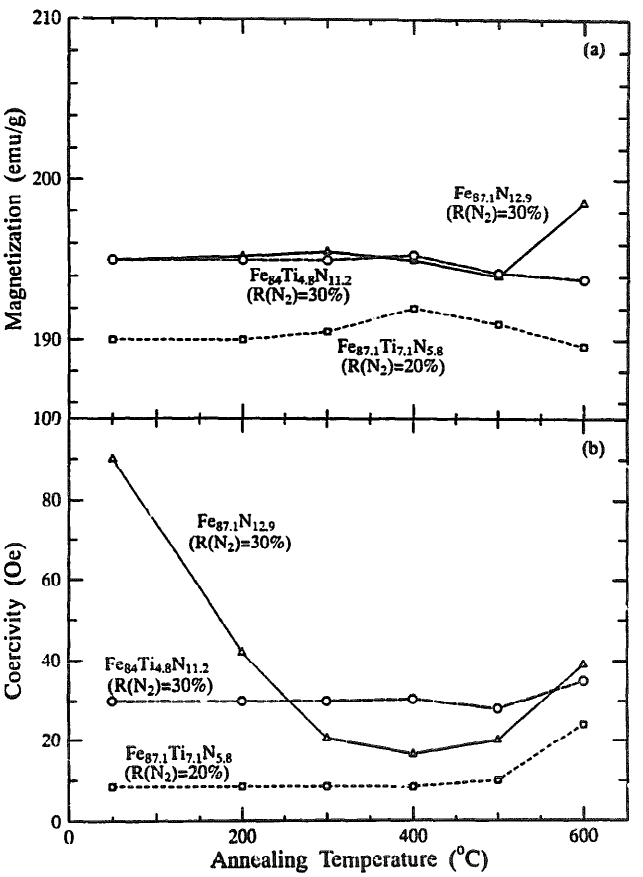

Fig. 7. Dependence of saturation magnetization M_s (a) and Coercivity H_c (b) on annealing temperature for the Fe–Ti–N films deposited at $R(N_2)=20$ and 30% and Fe–N film deposited at $R(N_2)=20\%$.

structure of the film as increasing annealing temperature (Fig. 3). No evidence has been found for Fe–N compounds in the deposited Fe–Ti–N films up to $R(N_2)=30\%$. A sufficient amount of Ti seems to inhibit the formation of iron nitride phases on annealing. The peak broadening with increases $R(N_2)$ could be due to the small grain size and peak splitting associated with the tetragonal distortion of α-Fe by interstitial nitrogen atoms.

The formation of the γ′-Fe_4N phase can have been observed in annealed Fe–N film deposited at the lower $R(N_2)=10\%$ (Fig. 2). In the Fe–Ti–N films, on the other hand, there is no observable change in the structure after annealing at 400 °C for 1 h (not shown here). This demonstrates the good thermal stability in the magnetic properties in the Fe–Ti–N films.

As shown in Fig. 4, the change of the lattice constant in the Fe–N films corresponds to the phase transformation from the α-Fe phase to the *bct* martensite (α′). Therefore, it is easily understood that the incorporation of nitrogen atoms results in lattice distortion of the α-Fe phase and causes a monotonic increase in H_c with increasing $R(N_2)$ for the as-prepared Fe–N films (Fig. 5(b)). For the as-prepared Fe–Ti–N films, however, the H_c first decreases and then increases with increasing (N_2) (Fig. 5(a)). This is ascribed to distortion of α-Fe lattice due to doping of Ti atoms and compressive stress caused by the incorporation of sufficient nitrogen atoms [16].

Fig. 7(a) and (b) show the dependence of the saturation magnetization M_s and coercivity H_c on T_A for the Fe–Ti–N and Fe–N films. In the Fe–Ti–N films, H_c shows almost no change for $T_A<500$ °C and slightly increases for $T_A=600$ °C because the grain size grows obviously (as shown Fig. 3). In the Fe–N film, on the other hand, the H_c first decreases drastically and then increases with increasing T_A. The decrease in H_c is ascribed to reduction of compressive stress due to formation of the γ′-Fe_4N phase. The increase in H_c results from the grain growth. The variation in M_s for both Fe–Ti–N and Fe–N films is not obvious below 500 °C and the increase of M_s of the Fe–N films after annealing at 600 °C is ascribed to decomposition of the γ′-Fe_4N phase.

5. Conclusions

The effects of heat treatment on the structure and magnetic properties of the Fe–Ti–N and Fe–N films prepared under the same deposition condition have been investigated. The large amount of Ti doping into Fe–N

film suppresses the formation of iron nitride phases even after annealing at 600 °C and expands the bcc lattice. For the Fe–Ti–N films, there is a tendency of forming amorphous phase as increasing $R(N_2)$ and the Ti_2N phase is formed at $R(N_2)$=30%. Compared with the Fe–Ti–N films, the formation of the γ'-Fe_4N phase in the Fe–N films before and after annealing and the decomposition of the γ'-Fe_4N phase cause a poor thermal stability in the magnetic properties in the Fe–N films. The decomposition temperature of the γ'-Fe_4N phase in non-equilibrium Fe–N films is about 570 °C. The second magnetic transformation temperatures are 540 °C in the Fe–Ti film and 440 °C in the Fe–N films.

Acknowledgments

The authors express their appreciation to Dr. T. Takada for his asistance with ICP analysis.

References

[1] M. Komuto, Y. Kozono, M. Hanazono, Y. Sugita, J. Appl. Phys. 67 (1990) 5126.
[2] K. Nakajima, S. Okamoto, J. Appl. Phys. 65 (1989) 4357.
[3] K. Nakajima, S. Matsumoto, Appl. Phys. Lett. 56 (1990) 92.
[4] S. Wang, M.H. Kryder, J. Appl. Phys. 67 (1990) 5134.
[5] A. Morisako, M. Matsumoto, M. Naoe, J. Appl. Phys. 69 (1991) 5619.
[6] H. Jiang, K. Tao, H.D. Li, J. Appl. Phys. 78 (1995) 3299.
[7] H. Jiang, K. Tao, H.D. Li, J. Magn. Magn. Mater. 149 (1995) 358.
[8] M. Takahashi, T. Shimatsu, IEEE Trans. Magn. 26 (1990) 1485.
[9] N. Ishiwata, C. Wakabayashi, H. Urai, J. Appl. Phys. 69 (1991) 5616.
[10] K. Nakanishi, O. Shimizi, S. Yoshida, J. Magn. Soc. Jpn. 15 (1991) 371.
[11] K. Nago, H. Sakakima, K. Ihara, J. Magn. Soc. Jpn. 15 (1991) 365.
[12] J.C. Lin, L.J. Chen, C.J. Chen, IEEE Trans. Magn. 30 (1994) 3912.
[13] G. Qiu, E. Haftek, J.A. Barnard, J. Appl. Phys. 73 (1993) 6573.
[14] K. Teruhuma, M. Miyazaki, H. Kawashima, K. Terazono, J. Magn. Soc. Jpn. 14 (1990) 257.
[15] F. Sato, T. Miyazaki, J. Magn. Soc. Jpn. 20 (1996) 481.
[16] D.L. Peng, K. Sumiyana, M. Oku, D.X. Li, K. Suzuki, Phy. Sol. Stat.(a) 157 (1996) 139.
[17] H. Miyajima, J. Magn. Soc. Jpn. 15 (1991) 675.